NJC

ROYAL SOCIETY OF CHEMISTRY

PAPER

View Article Online
View Journal | View Issue

Cite this: *New J. Chem.*, 2025, **49**, 13089

Biosourced and metal-free synthesis of conjugated polymers: *b*PPV, *b*CN-PPV and *b*PPTzTz†

Louis-Philippe Boivin, [a] Mia Prud'homme,[a] Audrey Poitras,[a] William Dupont,[a] Mario Leclerc *[a] and David Gendron *[b]

Received 5th March 2025,
Accepted 25th June 2025

DOI: 10.1039/d5nj00992h

rsc.li/njc

The growing demand for sustainable materials has spurred interest in biosourced feedstocks and metal-free polymerization techniques for organic electronics. This study explores the synthesis of conjugated polymers using renewable succinic acid-derived monomers through environmentally benign polymerization methods. New pathways were developed to produce three biosourced polymers: poly(phenylene vinylene) (***b*PPV**), poly(cyano-PPV) (***b*CN-PPV**), and poly(thiazolo[5,4-*d*]thiazole) (***b*PPTzTz**) using Gilch polymerization, Knoevenagel condensation, and Ketcham polymerization, respectively. Comprehensive characterization of these polymers, including molecular weight, optical, electrochemical, and thermal properties, demonstrates their potential for organic electronics. The polymers exhibit high renewable atom content, with polymer ***b*PPV** achieving 100% of its atoms coming from succinic acid. This work highlights the feasibility of integrating biosourced monomers and sustainable polymerization strategies, advancing the development of environmentally responsible materials for organic electronics.

Introduction

Organic electronics is a field that has been attracting significant attention in recent years. As society increasingly prioritizes sustainability, there is a growing drive to reduce reliance on critical minerals and replace them with more abundant organic materials. However, the majority of materials used in organic electronics are still derived from non-renewable sources, primarily petroleum[1] and they are commonly prepared using palladium-mediated coupling methods such as Stille, Suzuki and direct arylation polymerization.[2,3] To address these challenges, it is crucial to identify sustainable sources of starting materials and to find suitable metal-free polymerization protocols.[4]

One promising alternative to fossil fuels is forest biomass, which consists of carbohydrates (such as cellulose and hemicellulose) and aromatics (such as lignin and tannins).[5] Both of these components can be processed into added value compounds.[6] Research into cellulosic-derived starting materials has primarily focused on furan-substituted DPP,[7] synthesized from succinic acid and furfural. Using lignin derived starting materials, significant progress has been made using vanillin for the synthesis of conjugated polymers. For instance, our group has previously reported the synthesis of heterocycle-substituted benzenes rings using vanillin as a precursor.[8] In a subsequent study, we demonstrated their potential by polymerizing them through DArP with diketopyrrolopyrrole (DPP) for transistor applications.[9] Additionally, the groups of Kayser[10] and Brochon[11] have also explored vanillin-based monomers for synthesizing partially bio-sourced conjugated polymers, employing metal-free polymerization methods in both cases.

Since the last decade, only a few metal-free polymerization protocols have been reported.[12] Most of these methods rely on the same principle: the condensation of various nucleophiles with carbonyl groups to form alkene derivatives, examples include the aldol condensation,[13] the Knoevenagel condensation,[14,15] the Horner–Wadsworth–Emmons reaction,[16] and polyazomethine synthesis.[17] However, other methods utilize a range of organic reactions to achieve conjugated polymers, such as Gilch polymerization,[18] the Ketcham reaction,[19] Yao *et al.*'s pyrazine construction,[20] and the multicomponent polymerization developed by Kayser *et al.*[10]

This study seeks to explore the adaptation of metal-free polymerization techniques to biosourced monomers derived from succinic acid, a renewable feedstock readily obtainable

[a] *Département de Chimie, Université Laval, Québec City, Québec G1V 0A6, Canada. E-mail: mario.leclerc@chm.ulaval.ca*
[b] *Cégep de Thetford, Kemitek, Thetford Mines Québec, G6G 0A5, Canada. E-mail: dgendron@kemitek.org*

† Electronic supplementary information (ESI) available: Materials, full experimental details and characterisation. See DOI: https://doi.org/10.1039/d5nj00992h

from cellulose.[21] By employing dimethyl succinate, we developed novel pathways to conjugated polymers with distinct properties and high renewable atom content. Our approach resulted in the synthesis of three biosourced polymers: poly(phenylene vinylene) (***b*PPV**), cyano-PPV (***b*CN-PPV**), and poly(thiazolo[5,4-*d*]thiazole) (***b*PPTzTz**), *via* Gilch polymerization, Knoevenagel condensation, and Ketcham polymerization, respectively.

This paper presents the synthetic methodologies, detailed characterization, and renewable atom content analyses for these polymers. By evaluating their structural, optical, electrochemical, and thermal properties, we aim to highlight the potential of those biosourced materials in reducing reliance on petroleum-based precursors while demonstrating interesting properties required for applications in organic electronics. Through this work, we demonstrate the feasibility of integrating renewable feedstocks into advanced materials development, paving the way for more sustainable approaches to the synthesis of conjugated polymers.

Results and discussion

Knowing the different metal-free polymerization methods, we began investigating how to adapt some of these protocols to biosourced monomers to make useful conjugated polymers. Our search stopped on poly(phenylene vinylenes) (PPVs), which are a class of conjugated polymers that have been extensively studied and continue to be investigated for their applications in polymer light-emitting diodes (PLED) devices.[22] They have also been synthesized by a few metal-free polymerization methods (Gilch, Knoevenagel condensation, Horner–Wadsworth–Emmons reaction).[23] As shown in Scheme 1, the Gilch polymerization requires a monomer bearing two halomethyl groups, the Knoevenagel condensation involves the nucleophilic addition of a carbon atom bearing acidic hydrogen atoms to a carbonyl group and the Horner–Wadsworth–Emmons reaction is the condensation of a stabilized phosphonate carbanion on an aldehyde.

We oriented our search towards suitable starting materials that can be obtained from biomass. A publication from Short *et al.* describes that succinic esters could be dimerized and further aromatized into dimethyl 2,5-dihydroxyterephthalate, which features two ester groups.[24] These ester groups could then be converted into a variety of functional groups (halomethyl groups, aldehydes groups, nitrile groups, *etc.*) suitable for different metal-free polymerization protocols. However, we decided to avoid the Horner–Wadsworth–Emmons reaction as it required more synthetic steps to reach the targeted compound than the Gilch and Knoevenagel condensation.

The detailed synthetic procedures can be seen in the ESI,† as well as the ^{1}H and ^{13}C NMR spectra of new intermediate compounds in Fig. S16–S32 (ESI†).

Synthesis of biosourced poly(phenylene vinylene) (*b*PPV)

The first polymer we aimed to synthesize was polymer ***b*PPV** using the Gilch polymerization method.[25] The synthesis of the required dihalomethyl benzene monomer and further polymerization to ***b*PPV** is illustrated in Scheme 2. The first step involves the preparation of compound **1** (96% yield) *via* the Claisen condensation of succinic ester using NaH as reagent.[26] Compound **1** is then aromatized into compound **2** using *N*-chlorosuccinimide (NCS) as the oxidant, achieving a 85% yield.[24] The resulting yellow solid was alkylated with 2-ethylhexyl bromide in the presence of K_2CO_3 to produce compound **3** with a 60% yield.[27] Next, the ester groups present in compound **3** were reduced to alcohol groups using $LiAlH_4$, yielding compound **4** with a 96% yield.[28] The alcohol groups in compound **4** are subsequently converted to chlorines, thus forming the final monomer (compound **5**) with an 80% yield.[29] Compound **5** was then polymerized *via* the Gilch pathway to obtain polymer ***b*PPV**.[25] To prevent rapid gelation, *t*BuOK was added only after the solution of compound **5** in THF had been cooled to −78 °C, and the mixture was gradually heated to 50 °C. The reaction was quenched by precipitating polymer ***b*PPV** in MeOH at room temperature, followed by purification *via* Soxhlet extraction with MeOH, acetone, hexanes, and $CHCl_3$. The yield of polymer ***b*PPV** in the $CHCl_3$ fraction was found to be 51%.

Synthesis of polymer biosourced poly(cyano-PPV) (*b*CN-PPV)

We then aimed for the synthesis of polymer ***b*CN-PPV** by the Knoevenagel condensation. CN-PPVs are also of interest for

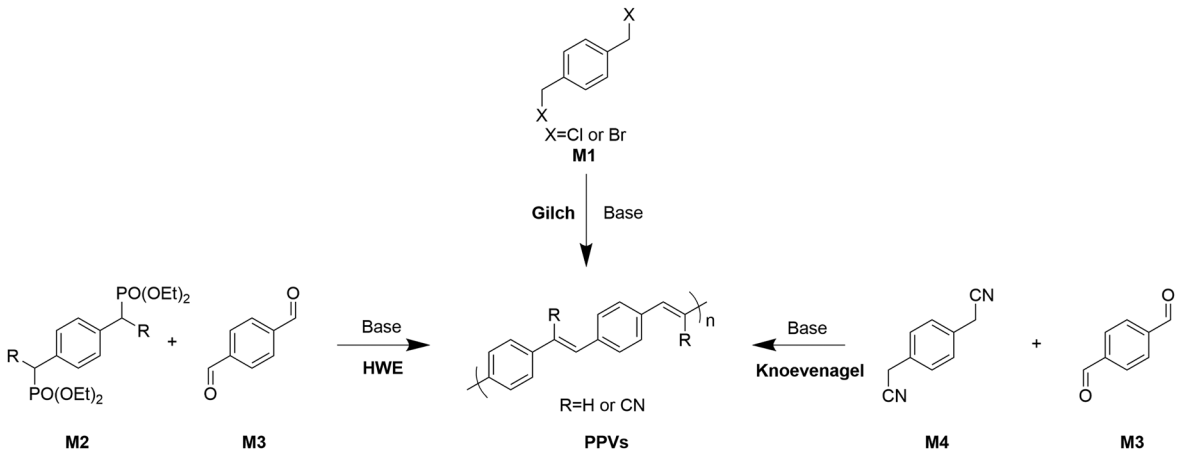

Scheme 1 Synthesis of PPVs by Gilch polymerization, Knoevenagel condensation and Horner–Wadsorth–Emmons reaction (HWE).

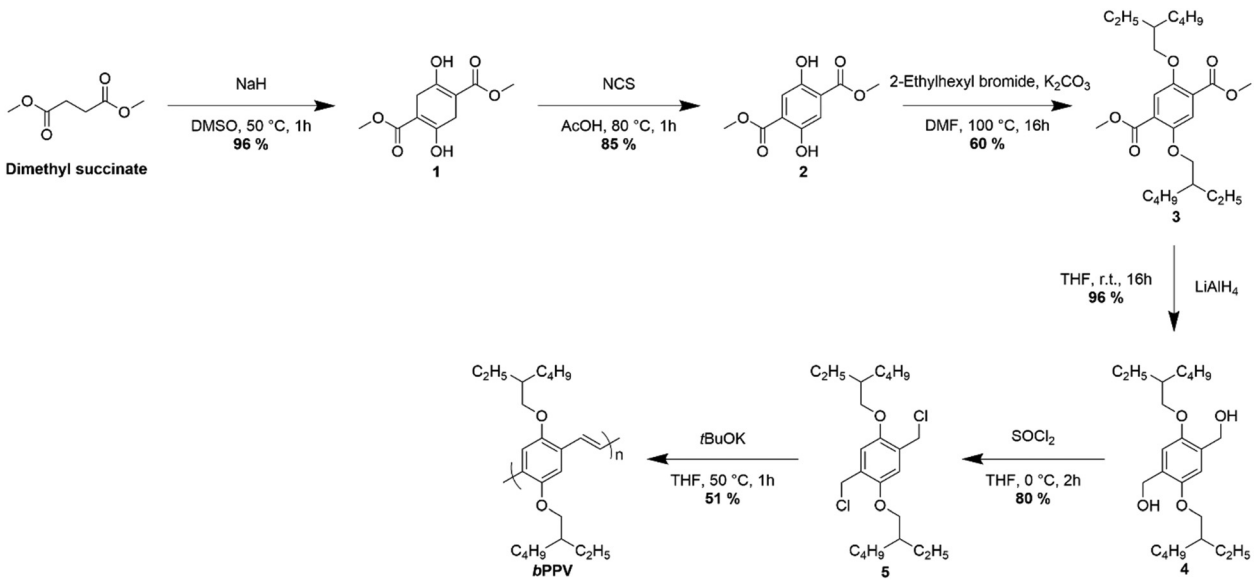

Scheme 2 Synthesis of polymer ***b*PPV**.

PLED application, as they have been shown to improve electron injection and charge captured at the interface in multilayer PLED devices which improves the overall device performance.[30] As illustrated in Scheme 3, we synthesized the dialdehyde compound **7** through the oxidation of compound **4** using pyridinium chlorochromate (PCC), achieving a 98% yield.[28] The dinitrile compound **6** was prepared by reacting dichloride **5** with NaCN, resulting in a 46% yield.[31] With both the nucleophile and electrophile in hand, we followed the protocol described by Thompson *et al.* for the Knoevenagel condensation.[31] Equimolar quantities of the monomers were mixed in anhydrous THF and anhydrous *t*BuOH, and the mixture was brought to reflux before adding 2.2 equivalents of *t*BuOK. Adding the base at high temperatures is crucial to

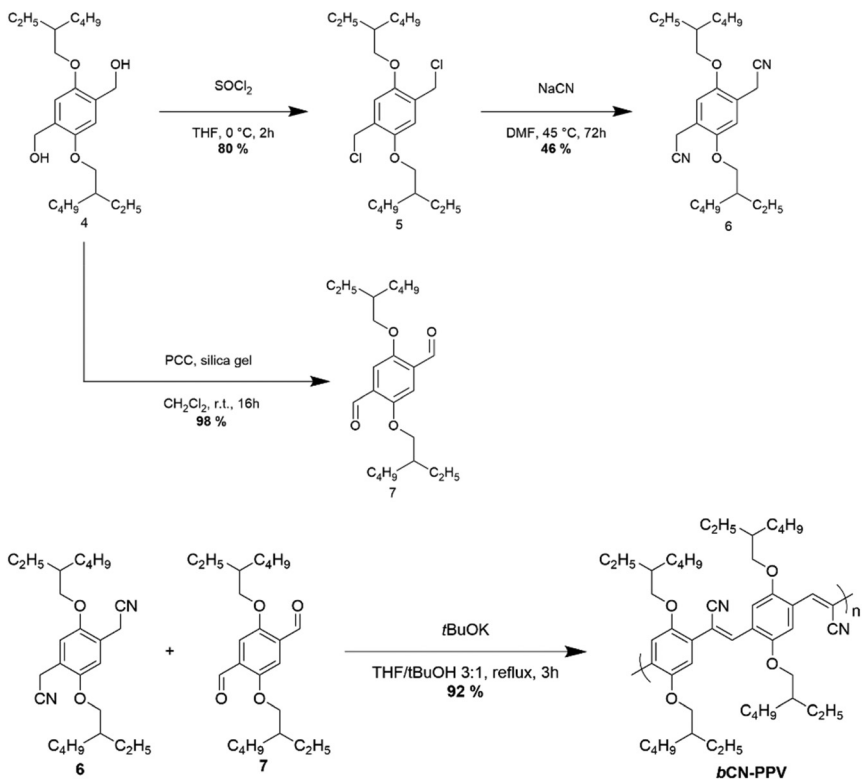

Scheme 3 Synthesis of polymer ***b*CN-PPV**.

minimize side reactions, such as the Thorpe–Ziegler reaction and Michael addition.[32,33] Upon completion of the Knoevenagel condensation, the polymer was precipitated in methanol at room temperature with the addition of two drops of AcOH and further purified *via* Soxhlet extraction using MeOH and acetone. The resulting polymer ***b*CN-PPV** was soluble in the acetone fraction and was obtained with a 92% yield.

Synthesis of polymer biosourced poly(thiazolo[5,4-*d*]thiazole) (*b*PPTzTz)

The synthesis of the dialdehyde compound **7**, used in the synthesis of polymer ***b*CN-PPV**, also enabled the preparation of other conjugated polymers, such as thiazolothiazoles (TzTz).

TzTz units have shown great potential in organic electronic. Indeed, they are more electron deficient than their thiophene counterpart which improve the oxidation stability, and they also show strong π–π interaction at the solid state which generally improve charge carrier mobility.[34,35] As illustrated in Scheme 4, according to the protocol of Lolaeva *et al.*, the dialdehyde was polymerized into polymer ***b*PPTzTz** using dithiooxamide in DMF under microwave heating.[19] Initially, we used ethylhexyl side chains, but due to the poor solubility of the resulting material, we opted to increase their length to decyltetradecyl side chains. To achieve this, we modified the previously used procedure for synthesizing compound **7** to incorporate the longer side chains, successfully obtaining monomer **8** with a 75% yield over the three steps from compound **2**. Dialdehyde **8** was then polymerized using the Ketcham polymerization method. The resulting polymer was precipitated in methanol and purified *via* Soxhlet extraction using methanol, acetone, and hexanes. The polymer dissolved in the hexanes fraction and after evaporation of the solvent, polymer ***b*PPTzTz** was obtained with a 90% yield.

Renewable atoms content

To evaluate the renewability of the biobased polymer obtained in this study, we performed calculations based on the method described by Dupont *et al.*[9] Specifically, we calculated both the $\%_{BioT}$, which represents the number of biosourced atoms divided by the total number of atoms in the polymer structure, and the $\%_{BioC}$, which excludes the alkyl side chains and considers only the atoms in the polymer core. Both values provide valuable insights: $\%_{BioT}$ considers the entire polymer structure, including the side chains, which may not always be biosourced, while $\%_{BioC}$ excludes the side chains to avoid an overestimation of renewability caused by simply increasing the length of the side chains.

Table 1 Renewable atom content of polymers ***b*PPV**, ***b*CN-PPV** and ***b*PPTzTz**

Polymer	$\%_{BioT}$	$\%_{BioC}$
***b*PPV**	100	100
***b*CN-PPV**	96.9	86.7
***b*PPTzTz**	96.3	66.7

In our case, the side chains were also biosourced. Both 2-ethylhexyl bromide and 11-(bromomethyl)tricosane were synthesized from their respective alcohols.[36] These alcohols, in turn, are produced *via* the Guerbet reaction using linear alcohols, which are commonly biosourced either from oils and fats (*e.g.*, palm oil, coconut oil)[37–39] or by fermentation.[40]

As shown in Table 1, polymer ***b*PPV** consists entirely of atoms (100%) derived from a renewable source (succinic acid). For polymer ***b*CN-PPV**, slightly lower but still high percentages of 96.9% and 86.7% were achieved, with and without including the side chains, respectively. The decrease is due to the inclusion of the nitrile group necessary for the Knoevenagel polymerization, which is not biosourced. For polymer ***b*PPTzTz**, the percentages were 96.3% and 66.7%, with and without the side chains, respectively. This result is expected, as the dithiooxamide required for forming the thiazolothiazole ring in the Ketcham reaction is not biosourced. These findings highlight the importance of considering both metrics. While the $\%_{BioT}$ values for polymer ***b*PPTzTz** and polymer ***b*CN-PPV** are similar due to the longer side chains present in polymer ***b*PPTzTz**, the $\%_{BioC}$ metric reveals a significant difference. Polymer ***b*PPTzTz** contains 20% fewer biosourced atoms than polymer ***b*CN-PPV** when the side chains are excluded.

Polymer characterization and thermal properties

The polymers were first characterized using ^{1}H NMR, FTIR spectroscopy, and SEC analysis. The yields and SEC data are summarized in Table 2. Polymer ***b*PPV** was obtained from the $CHCl_3$ fraction with a yield of 51%, polymer ***b*CN-PPV** from the acetone fraction with a yield of 92%, and polymer ***b*PPTzTz** from the hexanes fraction with a yield of 90%. For polymer ***b*PPV**, the lower yield of 51% can be attributed to discarding both the hexanes fraction and the insoluble polymer remaining in the Soxhlet thimble after $CHCl_3$ washing.

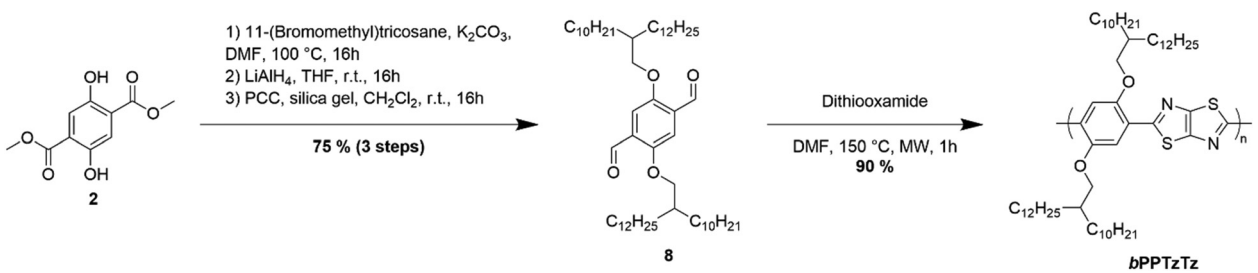

Scheme 4 Synthesis of polymer ***b*PPTzTz**.

Table 2 Polymerization yield, number-average molecular weights (M_n), mass-average molecular weight (M_w), polydispersity index (PDI), temperature of decomposition (T_d) and glass transition temperature (T_g) of all the polymers

Polymer	Yield (%)	M_n (kDa)	M_w (kDa)	PDI	T_d (°C)	T_g (°C)
***b*PPV**	51	370	1300	3.5	395	80
***b*CN-PPV**	92	7	21	3.0	400	35
***b*PPTzTz**	90	12	16	1.3	370	—

The molecular weights of the polymers were determined using SEC analysis in 1,2,4-trichlorobenzene (TCB). Polymer ***b*PPV** shows a high M_n of 370 kDa and an M_w of 1300 kDa, resulting in a PDI of 3.5. Achieving a high molecular weight is often a problem in Gilch polymerization due to lack of solubility,[41] but the polymer obtained remained soluble in THF, 2-MeTHF, $CHCl_3$, and TCB.

For polymer ***b*CN-PPV**, synthesized *via* Knoevenagel condensation, the M_n was measured to be 7 kDa, and the M_w was 21 kDa, with a PDI of 3.0. These lower molecular weights align with literature reports and are likely due to side reactions such as the Thorpe–Ziegler condensation and Michael addition, which alter the monomer ratios and hinder polymer chain growth.[32,33] Lastly, for polymer ***b*PPTzTz**, synthesized using the Ketcham polymerization, a M_n of 12 kDa and a M_w of 16 kDa were obtained, giving a PDI of 1.3. These results are consistent with previous results in the literature.[19] However, the molecular weight was likely limited by poor solubility in *N,N′*-dimethylformamide (DMF), as the polymer precipitated during the reaction.

Thermogravimetric analysis (TGA) and differential scanning calorimetry (DSC) were performed on each of the polymers (see Table 2 and Fig. S1–S4, ESI†). Polymers ***b*PPV**, ***b*CN-PPV**, and ***b*PPTzTz** exhibited high thermal stability, with a 5% weight loss occurring at 395 °C, 400 °C, and 370 °C, respectively. DSC measurements were conducted on each sample at heating rates of 20 °C min^{-1} and 5 °C min^{-1} to scan for thermal transitions such as the glass transition temperature (T_g) and the temperature of fusion (T_f), respectively. Polymer ***b*PPV** showed a T_g of 80 °C, which is slightly higher than what is reported for similar polymer MEH-PPV that possesses a T_g of around 70 °C.[42,43] This increase may be due to the high molecular weight of ***b*PPV**. Polymer ***b*CN-PPV** displayed a T_g of 35 °C, which is consistent with literature.[44] Lastly, no thermal transitions were observed for polymer ***b*PPTzTz**. it is worth noting that, at slower scan rate (5 °C min^{-1}), no thermal transition corresponding to the T_f was observed for the three samples.

^{1}H NMR spectra of polymers ***b*PPV**,[45] ***b*CN-PPV**,[46] and ***b*PPTzTz**[47] (see Fig. 1 and Fig. S30–S32 in the ESI†) were analyzed and compared with similar reports in the literature.[45–47] For polymer ***b*PPV**, the signal at 7.55 ppm corresponds to the vinylene protons, while the signal at 7.23 ppm corresponds to the benzylic protons. Signals at 4.00 ppm and in the range of 1.85 to 0.92 ppm are attributed to the ethylhexyl side chains. For polymer ***b*CN-PPV**, the multiplet at 8.1–7.7 ppm, which integrates for three protons, corresponds to two protons on the benzene ring and one proton from the alkene group. The multiplet at 7.1–6.8 ppm corresponds to two protons on the other benzene ring. Signals between 4.2–3.6 ppm and 1.9–0.6 ppm are assigned to the alkyl side chains. Notably, signals at 6.56 ppm and 3.24 ppm have been attributed to the *cis*-conformation of polymer ***b*CN-PPV** in previous reports.[46] By integrating the signal at 3.24 ppm and comparing it to the signal at 4.2–3.6 ppm, the *cis*-conformation content

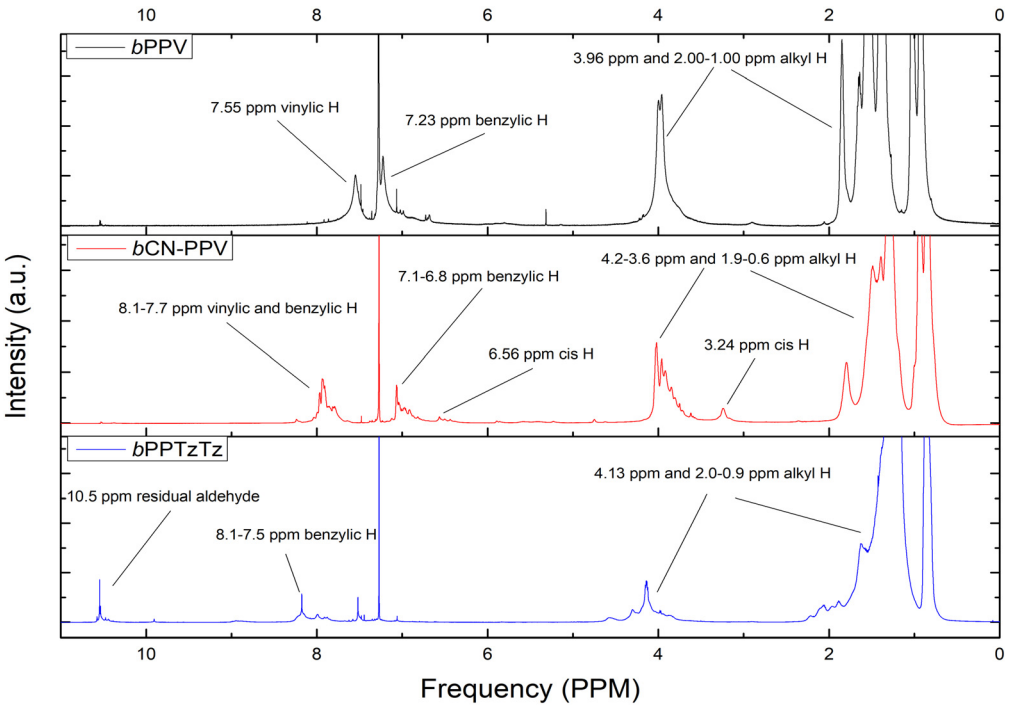

Fig. 1 NMR spectra of ***b*PPV**, ***b*CN-PPV** and ***b*PPTzTz**.

was estimated to be approximately 8%. For polymer ***b*PPTzTz**, the signal at 10.5 ppm corresponds to residual aldehyde end groups. Signals in the 8.1–7.5 ppm region correspond to protons on the benzene ring, while signals at 4.13 ppm and 2.0–0.9 ppm are assigned to the alkyl side chains.

The analysis by FTIR spectroscopy provided key insights into the structural features of polymers ***b*PPV**,[48] ***b*CN-PPV**[31] and ***b*PPTzTz**.[47,49] As shown in Fig. 2, for polymer ***b*PPV**, signals in the region of 2800–3100 cm^{-1} correspond to sp^2 and sp^3 C–H bond stretching, with the signal at 3060 cm^{-1} attributed to the *trans*-vinyl C–H stretch. Signals around 1500–1350 cm^{-1} correspond to semicircular phenyl stretching and alkyl CH_2 stretching. The signals at 1033 $cm^{-1}$and 1195 cm^{-1} are assigned to C–O stretching of the alkyl–O bond and the phenyl–O bond, respectively. Signals at 856 $cm^{-1}$and 969 cm^{-1} are attributed to out-of-plane wagging of the benzylic C–H and *trans*-vinyl C–H, respectively. For polymer ***b*CN-PPV**, signals in the 2800–3000 cm^{-1} region correspond to sp^3 and sp^2 C–H stretching. The signal at 2012 cm^{-1} corresponds to nitrile stretching, which is shifted to a lower wavenumber compared to the monomer (2250 cm^{-1}) due to conjugation with the vinylene groups formed during polymerization. Signals around 1500–1350 cm^{-1} correspond to semicircular phenyl stretching and alkyl CH_2 stretching. Signals at 1029 cm^{-1} and 1205 cm^{-1} are assigned to C–O stretching of the alkyl–O bond and the phenyl–O bond, respectively. For polymer ***b*PPTzTz**, sp^3 and sp^2 C–H stretching signals were observed between 2800–3000 cm^{-1}. A signal at 1684 cm^{-1} likely corresponds to residual aldehyde end groups, which are expected under the polymerization conditions used. The signal at 1604 cm^{-1} could correspond to the C=N stretching. Signals around 1400 cm^{-1} are assigned to C=C stretching vibrations within the aromatic ring. The signal at 1211 cm^{-1} corresponds to C–O stretching of the phenyl–O bond. Lastly, the signal at 1022 cm^{-1} is assigned to a combination of both the C–O alkyl stretching and the C–S stretching in the thiazolothiazole ring.

Optical and electrochemical properties

The optical absorption spectra were measured for each sample, both in solution in $CHCl_3$ and in thin films, which were spin-coated from a chloroform solution. The optical band gap ($E_{g\,optic}$) was calculated from the absorption onset in the thin film spectra. The ε_{max} was determined from a solution of the polymers in a known concentration following Beer–Lambert's law. The α_{max} was obtained from a spin-coated film of the polymers at a known thickness. The photoluminescence spectra were measured in solution in $CHCl_3$. To obtain the fluorescence quantum yield (φ_{fl}), we used the comparative method with a solution of rhodamine B in ethanol as our reference standard.[50] The electrochemical properties of the polymers were measured by cyclic voltammetry. The HOMO energy level was estimated from the onset of the oxidation wave, and the LUMO was determined from the onset of the reduction wave.[51]

The optical and electrochemical properties are shown in Table 3, Fig. 3 and in Fig. S5–S15 (ESI†). For polymer ***b*PPV**, the UV-Vis analysis and cyclic voltametric analysis showed an $\lambda_{max\,sol}$ at 510 nm and a slightly red-shifted $\lambda_{max\,film}$ at 520 nm, with an $E_{g\,optic}$ of 2.1 eV and an $E_{g\,elec}$ of 2.3 eV. At an excitation

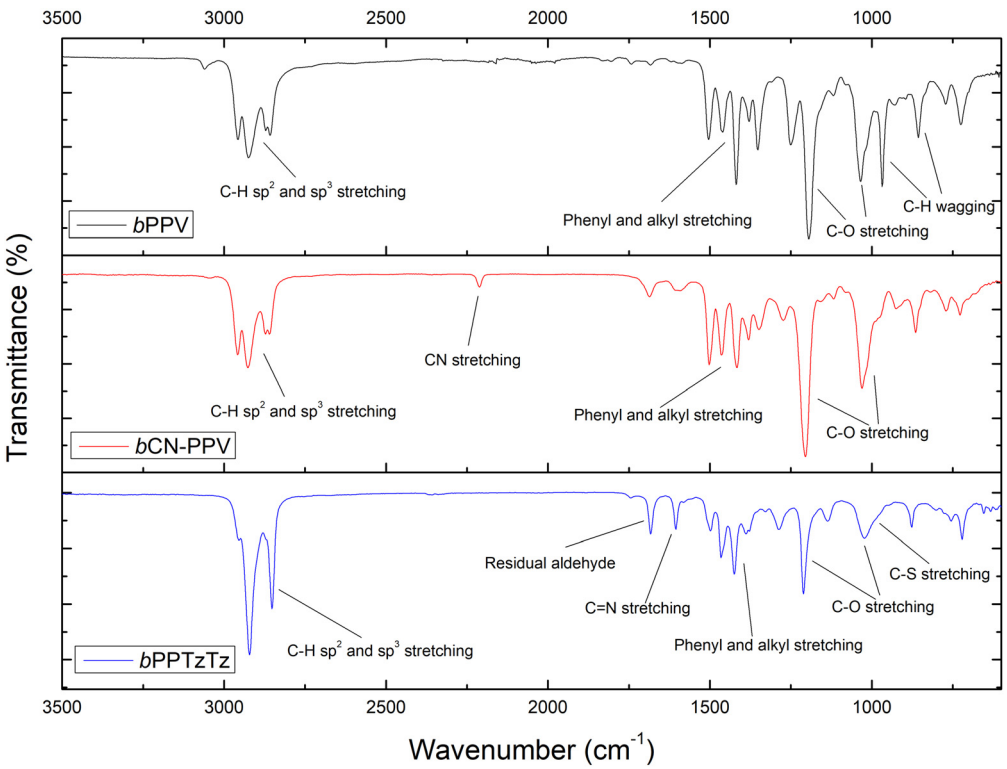

Fig. 2 FTIR spectra of ***b*PPV**, ***b*CN-PPV** and ***b*PPTzTz**.

Table 3 Optical and electronical properties of the polymers

Polymer	$\lambda_{max\,film}$ [a] nm	$\lambda_{max\,sol}$ [b] nm	$\lambda_{F\,max}$ [c] nm	$E_{g\,optic}$ [d] eV	$E_{g\,elec}$ [e] eV	ε_{max} [f] 10^4 M^{-1} cm^{-1}	α_{max} [g] 10^4 cm^{-1}	HOMO eV	LUMO eV	φ_{fl} [h] —
***b*PPV**	520	510	555	2.1	2.3	2.6	15	−5.0	−2.7	0.49
***b*CN-PPV**	450	450	555	2.3	2.3	1.7	9	−5.4	−3.1	0.20
***b*PPTzTz**	510	500	510	2.0	2.1	1.8	8	−5.5	−3.4	0.31

[a] Absorption maxima in thin films. [b] Absorption maxima in solution in $CHCl_3$. [c] Photoluminescence maxima in solution in $CHCl_3$. [d] Optical band gap from the thin film spectra. [e] Electronical band gap. [f] Molar absorption coefficient in $CHCl_3$. [g] Absorption coefficient in thin films. [h] Relative fluorescence quantum yield.

wavelength of 450 nm, polymer ***b*PPV** exhibited an $\lambda_{F\,max}$ of 555 nm and a φ_{fl} of 0.49. The HOMO and LUMO energy levels were estimated to be −5.0 eV and −2.7 eV, respectively. We also determined the ε_{max} to be 2.6 × 104 M^{-1} cm^{-1} and the α_{max} to be 15 × 104 cm^{-1}. This is consistent with data found in literature.[52–55] For polymer ***b*CN-PPV**, no shift in absorption maxima was observed between the solution and thin film spectra, both showing a λ_{max} of 450 nm, with an $E_{g\,optic}$ of 2.3 eV and an $E_{g\,elec}$ of 2.3 eV. At an excitation wavelength of 425 nm, an $\lambda_{F\,max}$ of 555 nm was obtained, resulting in a large Stokes shift of 105 nm, and a φ_{fl} of 0.20. The HOMO and LUMO energy levels were −5.4 eV and −3.1 eV, respectively. We also determined the ε_{max} to be 1.7 × 104 M^{-1} cm^{-1} and the α_{max} to be 9 × 104 cm^{-1}.This is mostly consistent with data found in literature, however, we did not observe a reversibility peak, so this result should be interpreted with caution.[52,53] It was noted that a lower φ_{fl} at 0.20 was obtained (0.35–0.4 in literature[52,53]), however it is hard to point to a specific explanation for this result as results found in literature typically have different side chains, molecular weight and/or methodology to obtain the φ_{fl}.[52,53] For polymer ***b*PPTzTz**, an $\lambda_{max\,sol}$ of 500 nm and a slightly red-shifted $\lambda_{max\,film}$ at 510 nm were observed, with an $E_{g\,optic}$ of 2.0 eV and an $E_{g\,elec}$ of 2.1 eV. Notable shoulders appeared at 460 nm and 540 nm on either side of the absorption maximum in the UV-Vis spectra of polymer ***b*PPTzTz**, which can be attributed to transitions at different vibrational levels from the ground state to the excited state. This effect is more pronounced in the photoluminescence spectra, where an

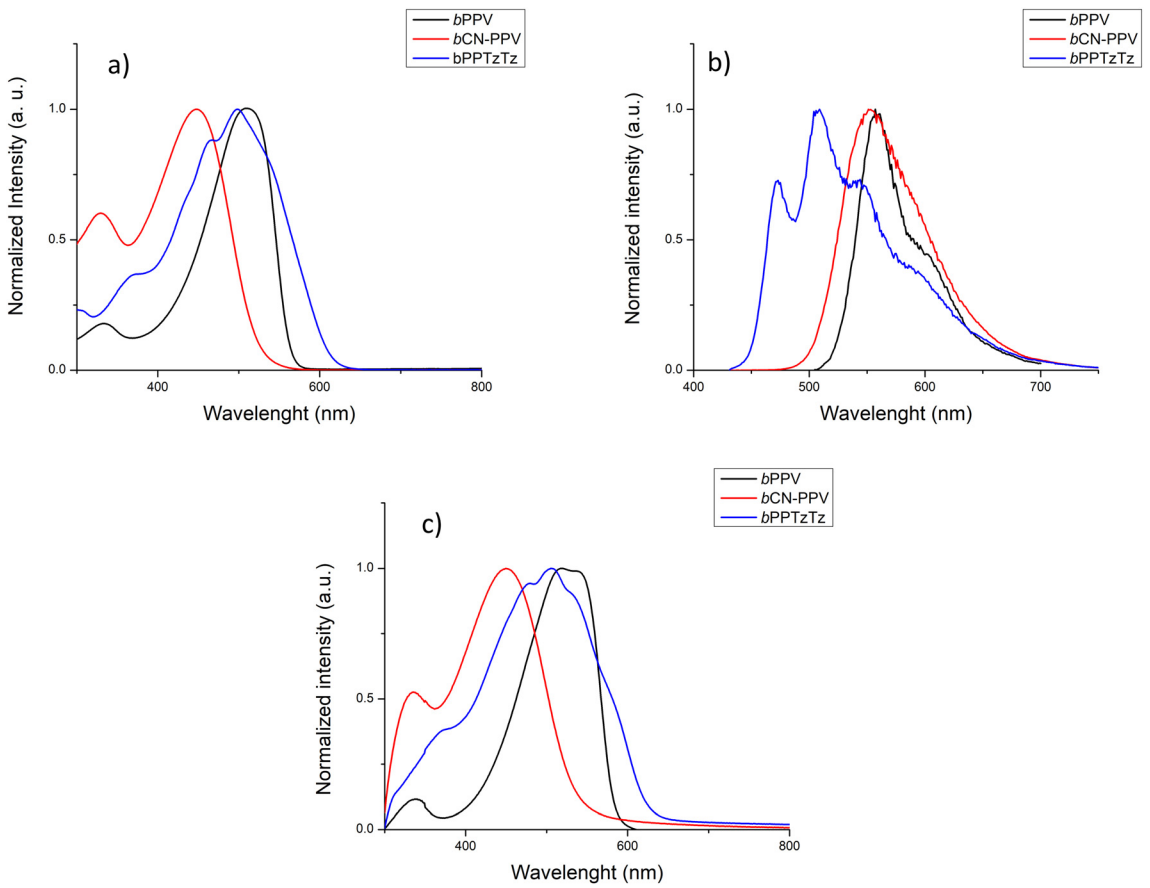

Fig. 3 (a) UV-Vis spectra in solution in $CHCl_3$, (b) photoluminescence spectra in solution in $CHCl_3$ and (c) UV-Vis spectra in thin films of polymers ***b*PPV**, ***b*CN-PPV** and ***b*PPTzTz**.

$\lambda_{F\,max}$ of 510 nm was obtained, with additional peaks at 470 nm and 550 nm, resulting from transitions from the excited state to the ground state at different vibrational levels. A φ_{fl} of 0.31 was obtained, and the HOMO and LUMO energy levels were −5.5 eV and −3.4 eV, respectively. We also determined the ε_{max} to be $1.8 \times 104\ M^{-1}\ cm^{-1}$ and the α_{max} to be $8 \times 104\ cm^{-1}$. There aren't precedents in the literature to compare the data obtained for ***b*PPTzTz**. Overall, the data highlight distinct optical and electrochemical characteristics for each polymer and show their potential for PLED applications.

Conclusions

In conclusion, this study demonstrates the viability of using forest biomass-derived materials, specifically succinic acid from cellulose, a renewable building block for the synthesis of conjugated polymers through three different metal-free polymerization methods. Three distinct polymers (***b*PPV**, ***b*CN-PPV**, and ***b*PPTzTz**) were successfully synthesized, characterized, and evaluated in terms of renewable content, optical, electrochemical, and structural properties.

The results highlight the potential of biosourced materials in reducing reliance on petroleum-based precursors while maintaining relevant properties for applications such as transistors and PLEDs. Notably, polymer ***b*PPV** achieved 100% biosourced atom content and suitable optical properties, while polymers ***b*CN-PPV** and ***b*PPTzTz** demonstrated high renewable atom percentages with distinct electronic and structural characteristics. These findings underline the feasibility of incorporating renewable resources and sustainable synthesis approaches in the development of advanced materials for organic electronics. Future efforts should focus on improving the renewability aspect of the reaction condition of the monomer synthesis (NaH, $SOCl_2$, PCC, DMF, halogenated solvents...), as the chemical industry reduces its dependence on petroleum-based, toxic and/or dangerous chemicals, but it is still marking a significant step toward the creation of fully renewable organic electronic devices.

Conflicts of interest

The authors declare no conflicts of interest.

Data availability

The data supporting the findings of this study (relative quantum yield study, synthesis of the monomers and polymers, UV-vis spectra of the polymer, photoluminescence spectra of the polymers, cyclic voltammograms of the polymers, thermogravimetric analysis and differential scanning calorimetry of the polymers as well as the ^1H and ^{13}C NMR of the intermediates and the ^1H NMR of the polymers) can be found in the ESI.†

Acknowledgements

The authors thanks Félix Gagnon for his knowledge on the obtention of the relative fluorescence quantum yields. The authors acknowledge the Fonds de Recherche du Québec, Nature et Technologies (FRQNT) Grant# 325901, for financial support (https://doi.org/10.69777/325901).

References

1 L.-P. Boivin, W. Dupont, D. Gendron and M. Leclerc, *Macromol. Chem. Phys.*, 2023, **224**, 2200378.
2 J.-R. Pouliot, F. Grenier, J. T. Blaskovits, S. Beaupré and M. Leclerc, *Chem. Rev.*, 2016, **116**, 14225–14274.
3 B. Chakraborty and C. K. Luscombe, *Angew. Chem.*, 2023, **135**, e202301247.
4 T. Kotnik and S. Kovačič, *Eur. J. Org. Chem.*, 2025, e202400874.
5 M. Norgren and H. Edlund, *Curr. Opin. Colloid Interface Sci.*, 2014, **19**, 409–416.
6 S. H. Shinde, A. Hengne and C. V. Rode, in *Biomass, Biofuels, Biochemicals*, ed. S. Saravanamurugan, A. Pandey, H. Li and A. Riisager, Elsevier, 2020, pp. 1–31.
7 C. H. Woo, P. M. Beaujuge, T. W. Holcombe, O. P. Lee and J. M. J. Fréchet, *J. Am. Chem. Soc.*, 2010, **132**, 15547–15549.
8 L.-P. Boivin, W. Dupont, M. Leclerc and D. Gendron, *J. Org. Chem.*, 2021, **86**, 16548–16557.
9 W. Dupont, L.-P. Boivin, M. Mainville, Y. Yuan, Y. Li, M. Leclerc and D. Gendron, *ACS Appl. Polym. Mater.*, 2025, **7**, 29–41.
10 L. V. Kayser, E. M. Hartigan and B. A. Arndtsen, *ACS Sustainable Chem. Eng.*, 2016, **4**, 6263–6267.
11 G. Garbay, L. Giraud, S. M. Gali, G. Hadziioannou, E. Grau, S. Grelier, E. Cloutet, H. Cramail and C. Brochon, *ACS Omega*, 2020, **5**, 5176–5181.
12 L. Giraud, S. Grelier, E. Grau, G. Hadziioannou, C. Brochon, H. Cramail and E. Cloutet, *J. Mater. Chem. C*, 2020, **8**, 9792–9810.
13 X. Zhu, J. Duan, J. Chen, R. Liu, Z. Qin, H. Chen and W. Yue, *Angew. Chem.*, 2024, **136**, e202311879.
14 N. C. Greenham, S. C. Moratti, D. D. C. Bradley, R. H. Friend and A. B. Holmes, *Nature*, 1993, **365**, 628–630.
15 K. Wu, P. Chen, T. Cui, B. Zhang, C.-L. Sun, J. Wang, X. Shao, L. Chen, Y. Chen and Z. Liu, *Macromol. Rapid Commun.*, 2025, **46**, 2401055.
16 L. Liao, Y. Pang, L. Ding and F. E. Karasz, *Macromolecules*, 2001, **34**, 7300–7305.
17 S. Barik and W. G. Skene, *Polym. Chem.*, 2011, **2**, 1091–1097.
18 J. D. Nikolić, S. Wouters, J. Romanova, A. Shimizu, B. Champagne, T. Junkers, D. Vanderzande, D. Van Neck, M. Waroquier, V. Van Speybroeck and S. Catak, *Chem. – Eur. J.*, 2015, **21**, 19176–19185.
19 A. V. Lolaeva, A. N. Zhivchikova, M. M. Tepliakova, M. V. Gapanovich, E. O. Perepelitsina, A. F. Akhkiamova, D. A. Ivanov, N. A. Slesarenko, A. G. Nasibulin, A. V. Akkuratov and I. E. Kuznetsov, *Mendeleev Commun.*, 2023, **33**, 682–685.
20 H. Yao, H. Huang, X. Zhang, N. Zhu and H. Bao, *Macromolecules*, 2024, **57**, 7165–7173.

21 S. Zhou, M. Zhang, L. Zhu, X. Zhao, J. Chen, W. Chen and C. Chang, *Biotechnol. Biofuels Bioprod.*, 2023, **16**, 1.
22 B. Van der Zee, Y. Li, G.-J. A. H. Wetzelaer and P. W. M. Blom, *Adv. Mater.*, 2022, **34**, 2108887.
23 A. J. Blayney, I. F. Perepichka, F. Wudl and D. F. Perepichka, *Isr. J. Chem.*, 2014, **54**, 674–688.
24 G. N. Short, H. T. H. Nguyen, P. I. Scheurle and S. A. Miller, *Polym. Chem.*, 2018, **9**, 4113–4119.
25 A. Banerji, A.-K. Schönbein and L. Halbrügge, *World J. Chem. Edu.*, 2018, **6**, 54–62.
26 Y. Zhang and J. Christoffers, *Synthesis*, 2007, 3061–3067.
27 G. I. Nosova, A. V. Yakimanskii, N. A. Solovskaya, E. V. Zhukova, R. Yu. Smyslov, A. R. Tameev, E. L. Aleksandrova and T. V. Magdesieva, *Polym. Sci., Ser. B*, 2011, **53**, 16–25.
28 H.-Z. Wang and H.-F. Chow, *ACS Appl. Polym. Mater.*, 2020, **2**, 1781–1789.
29 S.-L. Yim, H.-F. Chow, M.-C. Chan, C.-M. Che and K.-H. Low, *Chem. – Eur. J.*, 2013, **19**, 2478–2486.
30 D. R. Baigent, N. C. Greenham, J. Grüner, R. N. Marks, R. H. Friend, S. C. Moratti and A. B. Holmes, *Synth. Met.*, 1994, **67**, 3–10.
31 B. C. Thompson, Y.-G. Kim, T. D. McCarley and J. R. Reynolds, *J. Am. Chem. Soc.*, 2006, **128**, 12714–12725.
32 V. Boucard, *Macromolecules*, 2001, **34**, 4308–4313.
33 Y. Liu, G. Yu, Q. Li and D. Zhu, *Synth. Met.*, 2001, **122**, 401–408.
34 G. Reginato, A. Mordini, L. Zani, M. Calamante and A. Dessì, *Eur. J. Org. Chem.*, 2016, 233–251.
35 M. Ji, C. Dong, Q. Guo, M. Du, Q. Guo, X. Sun, E. Wang and E. Zhou, *Macromol. Rapid Commun.*, 2023, **44**, 2300102.
36 A. Jordan, R. M. Denton and H. F. Sneddon, *ACS Sustainable Chem. Eng.*, 2020, **8**, 2300–2309.
37 K. Noweck and W. Grafahrend, *Ullmann's Encyclopedia of Industrial Chemistry*, John Wiley & Sons, Ltd, 2006.
38 D. J. Anneken, S. Both, R. Christoph, G. Fieg, U. Steinberner and A. Westfechtel, *Ullmann's Encyclopedia of Industrial Chemistry*, John Wiley & Sons, Ltd, 2006.
39 C. Carlini, A. Macinai, A. M. Raspolli Galletti and G. Sbrana, *J. Mol. Catal. Chem.*, 2004, **212**, 65–70.
40 Z. Lin, W. Cong and J. Zhang, *Fermentation*, 2023, **9**, 847.
41 T. Schwalm, J. Wiesecke, S. Immel and M. Rehahn, *Macromol. Rapid Commun.*, 2009, **30**, 1295–1322.
42 C.-H. Chou, S.-L. Hsu, S.-W. Yeh, H.-S. Wang and K.-H. Wei, *Macromolecules*, 2005, **38**, 9117–9123.
43 S. Ashok Kumar, S. Gouthaman, J. S. Shankar, B. K. Periyasamy and S. K. Nayak, *Chem. Phys. Lett.*, 2021, **770**, 138462.
44 S.-A. Chen and E.-C. Chang, *Macromolecules*, 1998, **31**, 4899–4907.
45 N. Kamarulzaman, N. D. A. Aziz, R. H. Y. Subban, A. S. Hamzah, A. Z. Ahmed, Z. Osman, R. Rusdi, N. Kamarudin, N. S. Jumali and Z. Shaameri, 2011 3rd International Symposium & Exhibition in Sustainable Energy & Environment (ISESEE), 2011, pp. 63–68.
46 Y. Li, H. Xu, L. Wu, F. He, F. Shen, L. Liu, B. Yang and Y. Ma, *J. Polym. Sci., Part B: Polym. Phys.*, 2008, **46**, 1105–1113.
47 S. Halder, S. Pal, P. Sivasakthi, P. K. Samanta and C. Chakraborty, *Macromolecules*, 2023, **56**, 2319–2327.
48 M. Atreya, S. Li, E. T. Kang, K. G. Neoh, Z. H. Ma, K. L. Tan and W. Huang, *Polym. Degrad. Stab.*, 1999, **65**, 287–296.
49 D. Lin-Vien, N. B. Colthup, W. G. Fateley and J. G. Grasselli, *The Handbook of Infrared and Raman Characteristic Frequencies of Organic Molecules*, Elsevier, 1991.
50 A. M. Brouwer, *Pure Appl. Chem.*, 2011, **83**, 2213–2228.
51 N. Elgrishi, K. J. Rountree, B. D. McCarthy, E. S. Rountree, T. T. Eisenhart and J. L. Dempsey, *J. Chem. Educ.*, 2018, **95**, 197–206.
52 J. Sun, L. P. Sanow, S.-S. Sun and C. Zhang, *Macromolecules*, 2013, **46**, 4247–4254.
53 N. C. Greenham, I. D. W. Samuel, G. R. Hayes, R. T. Phillips, Y. A. R. R. Kessener, S. C. Moratti, A. B. Holmes and R. H. Friend, *Chem. Phys. Lett.*, 1995, **241**, 89–96.
54 K. Koynov, A. Bahtiar, T. Ahn, R. M. Cordeiro, H.-H. Hörhold and C. Bubeck, *Macromolecules*, 2006, **39**, 8692–8698.
55 Y. Nishikitani, D. Takizawa, H. Nishide, S. Uchida and S. Nishimura, *J. Phys. Chem. C*, 2015, **119**, 28701–28710.